Journal of Applied Physics

PERSPECTIVE | MAY 01 2024

Metastable structures of cation vacancies in semiconducting oxides

Special Collection: Defects in Semiconductors 2024

W. Beall Fowler ; Michael Stavola ; Andrew Venzie ; Amanda Portoff

J. Appl. Phys. 135, 170901 (2024)
https://doi.org/10.1063/5.0205665

Journal of Applied Physics PERSPECTIVE pubs.aip.org/aip/jap

Metastable structures of cation vacancies in semiconducting oxides

Cite as: J. Appl. Phys. **135**, 170901 (2024); doi: 10.1063/5.0205665
Submitted: 27 February 2024 · Accepted: 9 April 2024 ·
Published Online: 1 May 2024

W. Beall Fowler,[a] Michael Stavola, Andrew Venzie, and Amanda Portoff

AFFILIATIONS

Physics Department, Lehigh University, Bethlehem, Pennsylvania 18015, USA

Note: This paper is part of the special topic, Defects in Semiconductors 2024.
[a]**Author to whom correspondence should be addressed:** beall.fowler@lehigh.edu

ABSTRACT

The observed metastable characteristics of cation vacancies in Ga_2O_3 have prompted a wider search for such systems. In this Perspective, we consider a number of defect systems as candidates for metastability. Some of these are already known to have this property, while for others, this suggestion is new. The examples discussed here are but a sampling of a huge number of systems, and these are used to emphasize that the metastability of defect structures is both common and important; it may yield (for example) split vacancy equilibrium configurations and, hence, should be considered in developing defect models and in analyzing their properties.

I. BACKGROUND

Metastability—the phenomenon in which a system may exist for a measurable period of time in one or more configurations other than its state with the lowest free energy—is common in many length scales and in many types of systems. For example, on the atomic and molecular scales, configurational metastability, or isomorphism, is common in molecular systems, and in a larger scale, bulk condensed matter is found to exist in different crystalline and amorphous configurations.

It should not be surprising, then, to discover metastability in association with defects in non-metallic solids, and, indeed, this is the case. Such effects may be charge dependent as well as dependent on the details of the defect structure, such as the presence of trapped H^+. In most cases involving cation vacancies, favorable split vacancy–interstitial–vacancy configurations will involve high symmetry and will not generate an excess number of unsatisfied anion–cation bonds; simple chemical arguments may lead to insights. While not discussed here, the same may not be true for cation interstitials, where Coulomb repulsion may dominate and lead to low-symmetry split structures.

Both experimental and theoretical results are reviewed here, along with original theoretical results. The latter were obtained using the CRYSTAL17 code[1] to calculate the structures and properties by means of hybrid density functional theory with Gaussian basis functions in a supercell format. Details of these calculations are given in the Appendix. The resulting defect structures are illustrated using MOLDRAW[2] and POV-Ray.[3]

It must be recognized that this represents but a sampling, not only of defects but also of earlier work. Thus, for example, the recent work of Mosquera-Lois *et al.*[4] provides a detailed discussion of mechanisms leading to defect metastability and approaches for finding minimum-energy configurations, with examples other than the ones presented here.

II. SYSTEMS CONSIDERED

A. Molecular metastability

As one of a countless number of examples of molecular metastability, Fig. 1 shows the three isomorphic structures of C_3H_4: propadiene, propyne, and cyclopropene.[5] All three of these structures are stable under suitable conditions; the least stable, cyclopropane, transforms to propyne at 450 °C.

B. Vacancy-impurity in conventional semiconductors

While a suggestion[6] that the vacancy in Si would be found in a split vacancy–interstitial–vacancy configuration proved incorrect, Watkins[7] subsequently found that the complex of a substitutional Sn plus Si vacancy, indeed, forms a stable split configuration

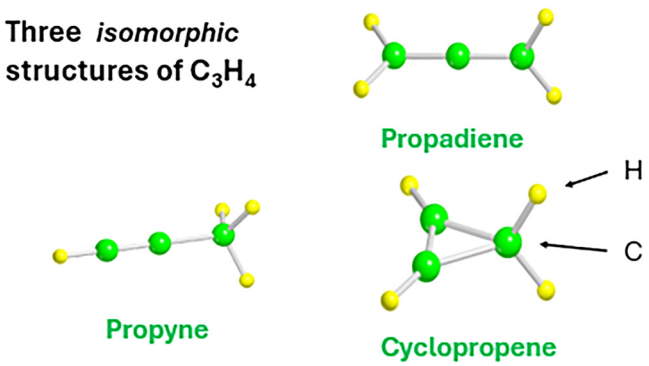

FIG. 1. The three isomorphic structures of C_3H_4: propadiene, propyne, and cyclopropene.

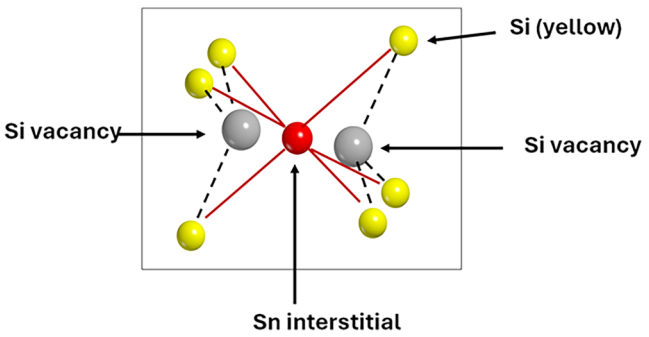

FIG. 2. Split Si vacancy plus substitutional Sn.

(Fig. 2). Furthermore, our calculations suggest that the unsplit configuration of this defect spontaneously relaxes to the split configuration—that is, it is not metastable. Here, the isolated Si vacancy has 4 unsatisfied bonds; the divacancy plus Sn interstitial is strongly favored as it satisfies all bonds with Sn in its common octahedral coordination. The same site for Si, which normally 4-coordinates, would not be chemically favorable; hence, the single Si vacancy remains unsplit.

It has also been found that a substitutional group IV impurity plus C vacancy in diamond forms split configurations,[8] with structures like that in Fig. 2 with the host Si replaced by C and the impurity Sn replaced by Si, Ge, Sn, or even Pb. Other split impurity-vacancy configurations in Si and Ge may also exist.[9,10] In addition, other metastable defects such as the DX center in GaAs have been thoroughly studied.[11] In some of these cases, the relative atomic size is likely to have an impact on the structure.

C. Oxygen vacancy (E′ centers) in α-quartz

While oxygen in α-quartz is twofold coordinated, the two silicon neighborhoods are inequivalent. This leads to the possibility[12] of trapped charge at an O vacancy being located preferentially on one of the two silicons. Indeed, the energetically favored structure of the positively charged O vacancy is found to involve a large, "puckered" relaxation of one Si^+, which can then form a back bond with a lattice oxygen, forming a three-coordinated, positively charged O[13–15] (Fig. 3). A remaining EPR-active electron[16] is trapped on the other Si. The low symmetry of the O site in this E_1' center means that this structure occurs only in one direction, and in other charge states, the puckered configuration is not favored.

Furthermore, this site inequivalence and the possibility of back-bonding lead to the possibility that two apparently distinct, H-related O vacancy defects (E_2' and E_4' centers) are, in fact, one defect in two isomorphic configurations.[17]

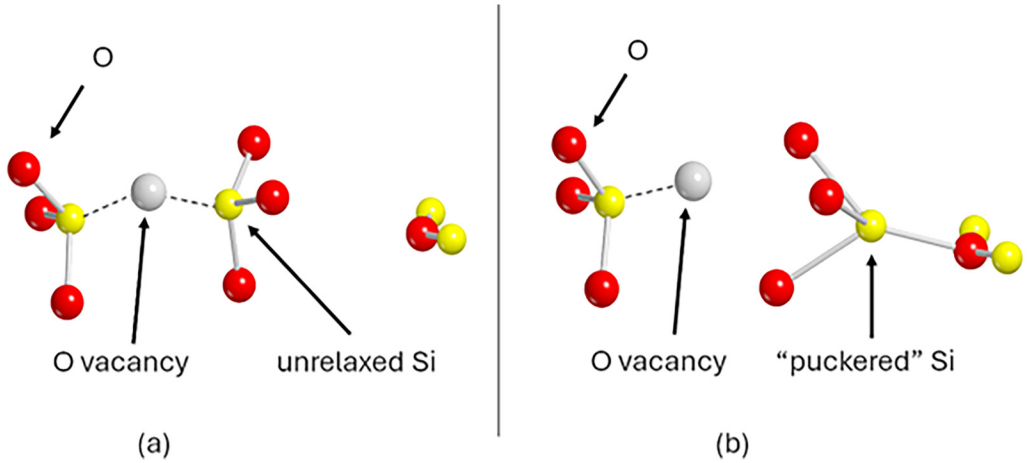

FIG. 3. Unrelaxed (a) and puckered (b) structure of the E_1' center in α-quartz.

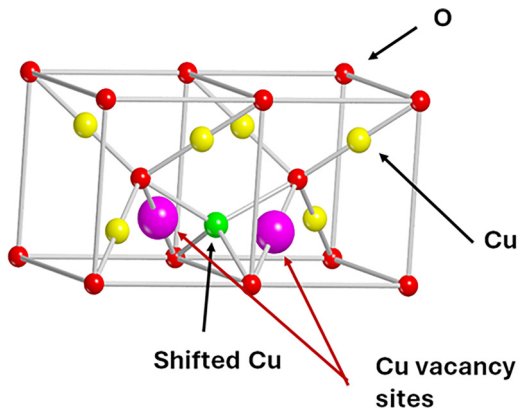

FIG. 4. Split Cu vacancy in Cu_2O.

D. Cu vacancy in Cu_2O

Cu_2O has a cubic lattice with fourfold coordinated O and twofold coordinated Cu. In this structure, there exists a fourfold coordinated interstitial site equally between two Cu sites, thus leading to the possibility of a split Cu vacancy–Cu interstitial–Cu vacancy configuration (Fig. 4). In this situation, the split site satisfies all Cu–O bonds, as the nature of the bonding changes from twofold to fourfold. Raman experiments provide evidence for the existence of this split configuration.[18] Early calculations[19,20] predicted different orderings of split vs simple configurations; later work by Isseroff and Carter[21] predicted that the unsplit configuration for the neutral vacancy is more stable by 0.21 eV. We have found, using CRYSTAL17, a similar result for the (−1) charge state, favoring the unsplit configuration by 0.33 eV. The detailed work of Isseroff and Carter predicts a localized hole for the split configuration (and, thus, a hole trap) and a delocalized hole for the simple vacancy, and suggests that both configurations may contribute to conduction in Cu_2O.

E. Cation vacancy in the rutile structure

Many oxides and several halides may be found in the rutile structure.[22] This structure is tetragonal; each cation has six anion neighbors, while each anion has three cation neighbors. In this structure, there exists a sixfold coordinated interstitial site equidistant from two cation sites in the a–b plane, a candidate for a split cation vacancy–cation interstitial–cation vacancy configuration (Fig. 5). We have investigated several of these—SnO_2, TiO_2, "stishovite" SiO_2, and MgF_2 using CRYSTAL17, and find that in all these cases that while the split configuration is metastable, it is disfavored energetically by ∼1–3 eV. Table I summarizes these results. While the split configuration maintains six unsatisfied cation-O bonds and octahedral coupling, cation-O distances are changed and the symmetry is reduced in that the cation-O directions are no longer mutually perpendicular. However, it should be noted that the sampling of results shown here is only a fraction of the compounds that may have this structure, including some with magnetic properties.

F. Brookite

Brookite[22] is a somewhat rare, orthorhombic structure found for TiO_2. We find that while a split cation vacancy–cation interstitial–cation vacancy configuration may exist, it is disfavored energetically by ∼2 eV in the neutral charge state. The split configuration appears to introduce considerable strain at the defect site.

G. Beta-tridymite

Tridymite[23] is a rare structure of SiO_2 that can be found in several phases. The beta phase, considered here, has a hexagonal symmetry [Fig. 6(b)]. Normal and split configurations for the Si

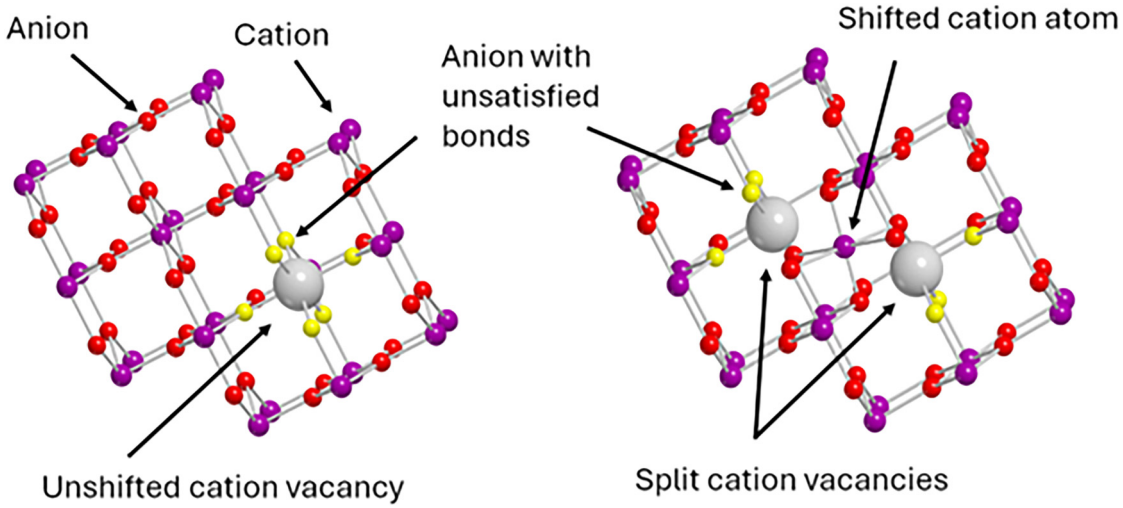

FIG. 5. Unsplit and split cation vacancy sites in the rutile structure, observed along the c axis.

TABLE I. Cation vacancy in the rutile structure. ΔE = E(split) – E(normal).

Material	Vacancy charge	ΔE (eV)	Favored
MgF_2	−2	+1.2	Normal
SiO_2	−4	+2	Normal
TiO_2	0	+2.4	Normal
SnO_2	−4	+2.4	Normal
SnO_2	−2	+2.9	Normal

vacancy are shown in Fig. 7. We find that the split configuration is favored energetically by 0.5 eV in the (−4) charge state. In this case, the Si shift reduces the number of unsatisfied Si–O bonds. Furthermore, the split configuration is of a higher symmetry than the normal vacancy site.

H. Corundum and anti-corundum structures

Sapphire, or corundum, or α-Al_2O_3, is a stable, well-known material that has many industrial applications[24] and has been widely studied. The less-common alpha phase of Ga_2O_3 has the same structure and is receiving considerable interest for its potential use in electronic and optical devices.[25] Many other oxides may be found in this structure family, including the oxides of magnetic materials, which we have not studied. Furthermore, materials are found to exist in the so-called anti-corundum structure,[26] such as Ca_3N_2. Here, the N occupies the nominal site of the cation, while the Ca occupies the O site.

In all these cases, the structure is quasi-hexagonal [Fig. 6(a)]. We have used vibrational spectroscopy to study H or D (deuterium) impurities located in samples consisting of α-Ga_2O_3 deposited on α-Al_2O_3 substrates,[27] These results combined with theory have led to the identification of H or D trapped at normal, or unsplit, cation vacancies in both oxides. However, our calculations on cation vacancies in the absence of H or D reveal the existence of a split configuration (Fig. 8) in both materials, which is energetically favored by 0.6–0.7 eV, as noted in Table II. This ordering had previously been predicted for α-Al_2O_3 by Lei and Wang.[28] The results are also shown in Table II for other oxides as well as for two anti-corundum examples. In most cases, the split configurations are found to be energetically favored. We note that the normal N vacancy site in Ca_3N_2 appears to be unstable, with relaxation into the split state occurring in the calculation.

Here, the number of unsatisfied cation-O bonds is the same in unshifted and split configurations. The split configuration is of a higher symmetry than the unshifted one. A subtle difference involves the nature of the cation-O bonds. In the unshifted configuration, the unshifted cation is bonded to three "closer" O (yellow) and three "farther" O (red), while in the shifted configuration, the cation has six "farther" O neighbors.

I. β-Ga_2O_3 and isostructural θ-Al_2O_3

Monoclinic[29] β-Ga_2O_3 is receiving considerable attention among the class of transparent conducting oxides for use in high-power, deep UV, and challenging environment applications.[30,31] As such, it has been the object of research and development for over a decade. A significant portion of this research has involved the study of O–H centers and is reviewed in a Tutorial by Stavola *et al.*[32] This work along with other studies has revealed important and interesting metastable properties of the Ga vacancy.

In 2011, Varley *et al.*[33] predicted the existence of the split Ga vacancy–Ga interstitial–Ga vacancy configuration shown in Fig. 9 as $V_{(Ga1)}$(c). Several years later, Krytsos *et al.*[34] indicated that at least two other split configurations could exist, one of which is shown in Fig. 9 as $V_{(Ga1)}$(b). [Both of these are configurations that

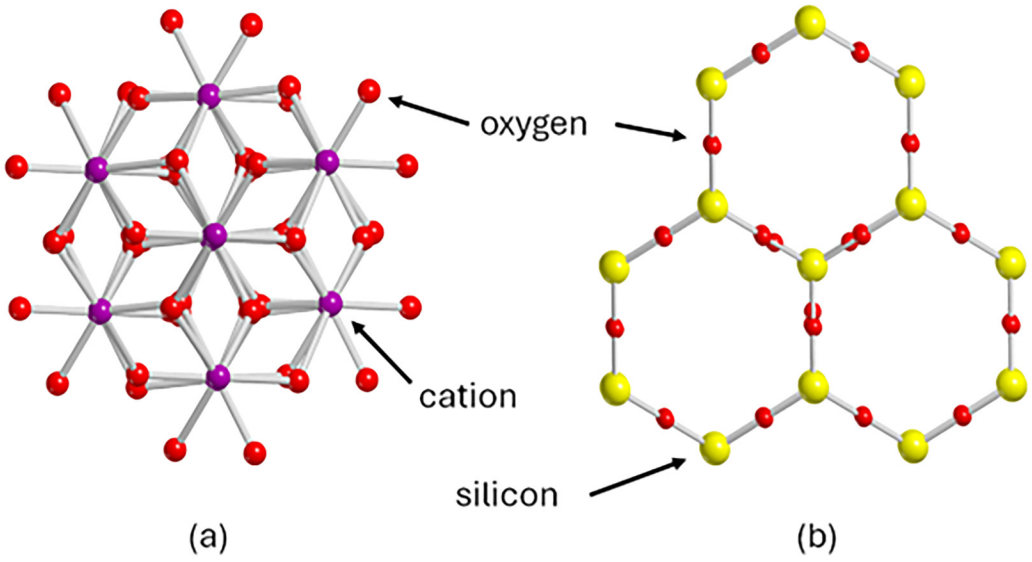

FIG. 6. Corundum (a) and beta-tridymite (b) structures viewed along the c axis.

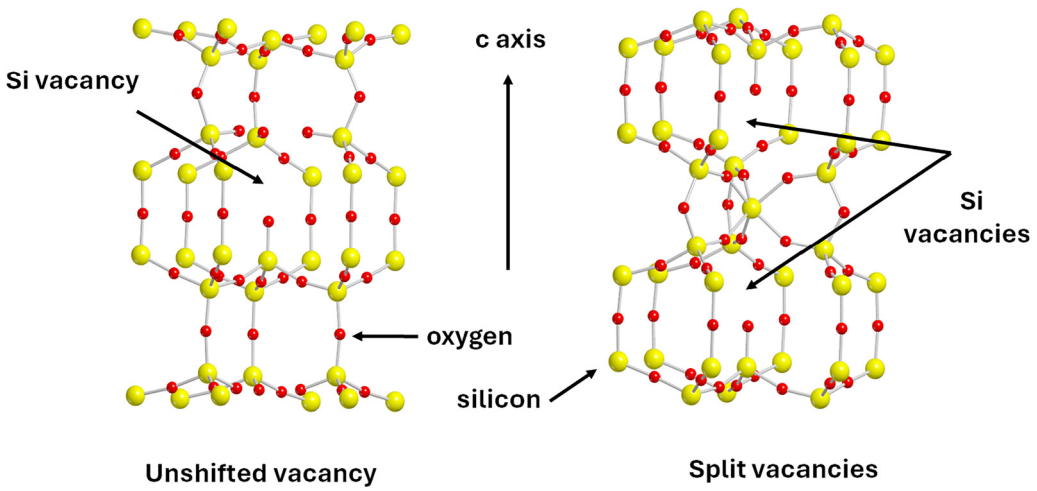

FIG. 7. Unsplit and split cation vacancy sites in the beta-tridymite structure.

involve shifts of only the tetrahedral Ga(1).] Subsequent[35,36] experimental and theoretical studies of the vibrational properties of O–H and O–D revealed the trapping of H or D on sites associated with both type (b) and type (c) split configurations. This work has continued and is thoroughly reviewed in Ref. 32.

Subsequent experimental work[37–40] has supported the existence of split Ga(1) vacancy structures as shown here. Both are strongly favored energetically over the unsplit version, by 0.6–1 eV. In both (b) and (c) configurations, the shifted Ga goes from 4-coordinated to 6-coordinated, reducing the number of unsatisfied Ga–O bonds from 4 to 2. The split configurations are also of higher symmetry than the unsplit. The relative stability of configuration (c) over (b) reflects the nature of the unsatisfied bonds; in (c), the oxygens are 3-coordinated, while in (b), they are 2-coordinated. Still, the unsplit version is predicted to be metastable, and in fact, it is predicted to be energetically favored when three or four H are trapped.[41] However, such decorated defects would have infrared signatures not experimentally observed, namely, transitions with polarization components in the (010) direction.

The solution of this puzzle is likely to involve the process of diffusion of the Ga(1) vacancy. In this structure, diffusion may readily occur within the [010] plane as the motion of the vacancy between the split sites (b) and (c) along the crystal c axis. It was predicted[41] that the energetically favored process would involve the coordinated motion of two Ga(1) atoms, as shown as the "intermediate" panel in Fig. 9, thus bypassing completely the unsplit site. Subsequent work by Frodason *et al.*[42] has shown in great detail that this process is, indeed, favored and that furthermore, the intermediate structure itself is metastable! Thus, the vacancy system may not exist in the unsplit state.

Θ-Al_2O_3 has the same monoclinic crystal structure[43] as does β-Ga_2O_3. We have carried out CRYSTAL17 calculations on Al vacancy defects in this system, mimicking the same calculations done for Ga vacancies in β-Ga_2O_3, and in virtually every respect, the outcomes map onto one another, with slightly different

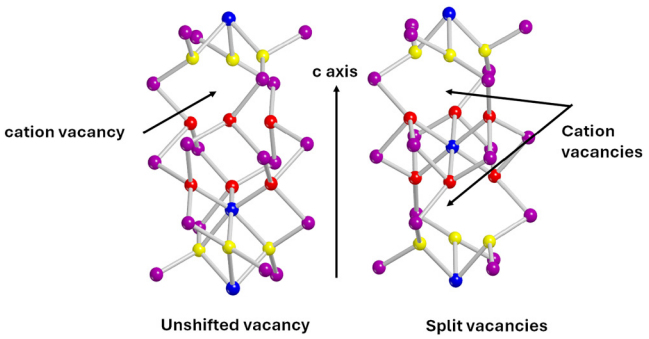

FIG. 8. Unsplit and split cation vacancy sites in the corundum structure. Sites are color coded as follows: cation, purple; cation along the central c axis, blue; O in a larger triangle, red; O in a smaller triangle, yellow.

TABLE II. Cation (anion) vacancy in the corundum (anticorundum) structures. ΔE = E(split) − E(normal).

Material	Vacancy charge	ΔE (eV)	Favored
α-Al_2O_3	−3	−0.7	Split
α-Ga_2O_3	−3	−0.6	Split
α-In_2O_3	−3	−0.6	Split
Ti_2O_3	−3	+1.9	Normal
Ti_2O_3	0	−1	Split
Mg_3N_2	+3	−0.8	Split
Ca_3N_2	+3	…	Split
α-Al_2O_3 + H^+	−2	+0.46	Normal
α-Ga_2O_3 + H^+	−2	+0.52	Normal

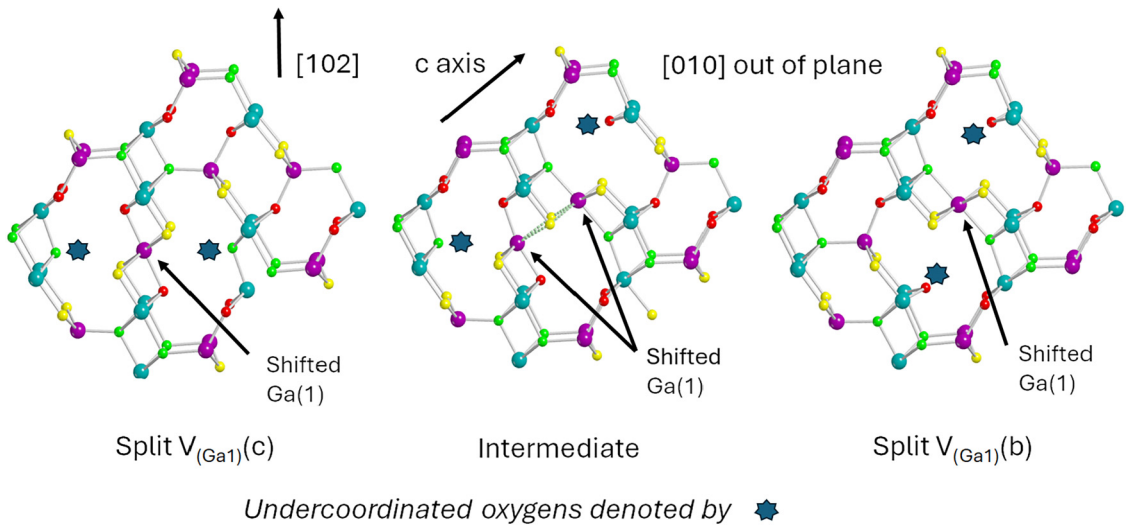

FIG. 9. Split Ga(1) vacancy sites in the β-Ga_2O_3 (and θ-Al_2O_3) structures. The inequivalent Ga and O sites are color coded by their coordination: tetrahedral Ga(1), purple; octahedral Ga(2), dark green; trigonal pyramidal O(1), red; trigonal planar O(2), yellow; tetrahedral O(3), light green.

magnitudes of structural relaxations and energies, but very similar outcomes. We have not considered the case of alloys of aluminum and gallium oxides in the β-Ga_2O_3 structure. The interest in these alloys for device applications suggests that potential split defect configurations could play a role.

III. SUMMARY

Presented here is a sampling of results on a variety of (mostly) oxide systems that serves to point out the importance of considering metastable cation defect structures, especially split configurations, for a proper understanding of defect properties. Systems with hexagonal or quasi-hexagonal structures, such as corundum, anti-corundum, and beta-tridymite, as well as those with the monoclinic β-Ga_2O_3 structure, appear to be particularly susceptible to have split cation vacancies in equilibrium.

As a sampling, these results leave open further work. Other oxide structures such as polymorphs of Ga_2O_3 or Al_2O_3, in particular, ones that contain cation vacancies in their basic structure, bear consideration. Systems such as VO_2, which undergoes a metal–insulator transition accompanied by a structural phase transition, may well have interesting properties associated with metastable cation vacancies. In addition, split configurations might be found in systems with magnetic properties, as well as the plethora of more complex oxides such as oxides with more than one cation constituent. It may well be that automated search processes, perhaps using artificial intelligence, would be useful in finding candidate systems.

ACKNOWLEDGMENTS

This work was supported by the National Science Foundation (NSF) (Grant No. 1901563). Portions of this research were conducted on Research Computing resources provided by Lehigh University and supported by the NSF award under Award No. 2019035.

AUTHOR DECLARATIONS

Conflict of Interest

The authors have no conflicts to disclose.

Author Contributions

W. Beall Fowler: Conceptualization (equal); Formal analysis (equal); Investigation (equal); Methodology (equal); Software (equal); Validation (equal); Visualization (equal); Writing – original draft (equal). **Michael Stavola:** Conceptualization (equal); Data curation (equal); Funding acquisition (equal); Investigation (equal); Project administration (equal); Visualization (equal); Writing – review & editing (equal). **Andrew Venzie:** Conceptualization (equal); Data curation (equal); Investigation (equal); Validation (equal); Writing – review & editing (equal). **Amanda Portoff:** Conceptualization (equal); Data curation (equal); Investigation (equal); Validation (equal); Writing – review & editing (equal).

DATA AVAILABILITY

The data that support the findings of this study are available from the corresponding author upon reasonable request.

APPENDIX: DETAILS OF CRYSTAL17 CALCULATIONS

The CRYSTAL17 code[1] was used for theoretical calculations at Lehigh University reviewed here. In such calculations, many choices may be made in terms of input conditions: basis set, hybrid exchange, charge state, supercell size, numerical tolerances, and so forth. While we have investigated from time to time the effects of

TABLE III. Basis set information.

Element	Type	Reference
H	3-11G*	45
N	6-21G*	46
O	8-411G	47
F	7-311G*	48
Mg	8-511G	49
Al	8-511G*	50
Si	66-21G*	51
Ca	86-511(3d)G	52
Ti	86-511(3d)G	53
Cu	86-4111(41d)G	54
Ga	86-4111(41d)G	55
Sn	ECP, 411(51d)	56

these conditions, for the most part we have found that the results obtained do not vary significantly as a result. Hence, for the most part we have used the same conditions in all calculations, with the expectation that if the conditions are "reasonable," internal consistency is important in allowing internal comparisons.

With this in mind, most of the results given here utilized default tolerances, the B3LYP hybrid exchange function,[44] ionic charge states, and supercell sizes of order 100 or more, with dimensions carefully chosen to reflect the geometries of the defects being investigated. The supercells of charged defects are neutralized by the addition of a uniform charge density, after which no further corrections are made in comparing the results for each configuration of interest in a given defect system. The basis sets used are tabulated in Table III. It should be noted that nearly all of these may be found on the CRYSTAL website: www.crystal.unito.it.

REFERENCES

[1]R. Dovesi, A. Erba, R. Orlando, C. M. Zicovich-Wilson, R. Civalleri, I. Maschio, M. Rérat, S. Casassa, J. Baima, S. Salustro, and B. Kirtman, Wiley Interdiscip. Rev.: Comput. Mol. Sci. **8**, e1360 (2018).
[2]P. Ugliengo, see http://www.moldraw.unito.it for "MOLDRAW (2006), a program to display and manipulate molecular and crystal structures."
[3]See http://povray.org for "POV-Ray."
[4]I. Mosquera-Lois, S. R. Kavanagh, A. Walsh, and D. O. Scanlon, npj Comput. Mater. **9**, 25 (2023).
[5]https://webbook.nist.gov/?chemistry/ (NIST Chemistry WebBook SRD 69)
[6]B. J. Masters, Solid State Commun. **9**, 283 (1971).
[7]G. D. Watkins, Phys. Rev. B **12**, 4383 (1975).
[8]T. Iwasaki, "Color centers based on heavy group-IV elements," in *Semiconductors and Semimetals*, edited by C. E. Nebel, I. Aharonovich, N. Mizuochi, and M. Hatano (Academic Press Inc., New York, 2020), Vol. 103, pp. 237–256.
[9]H. Höhler, N. Atodiresei, K. Schroeder, R. Zeller, and P. H. Dederichs, Phys. Rev. B **71**, 035212 (2005).
[10]N. Arutyunov, R. Krause-Rehberg, M. Elsayed, V. Emtsev, N. Abrosimov, G. Oganesyan, and V. Kozlovski, J. Phys.: Condens. Matter **33**, 245702 (2021).
[11]P. M. Mooney, J. Appl. Phys. **67**, R1 (1990).
[12]F. J. Feigl, W. B. Fowler, and K. L. Yip, Solid State Commun. **14**, 225 (1974).
[13]J. K. Rudra and W. B. Fowler, Phys. Rev. B **35**, 8223 (1987).
[14]K. C. Snyder and W. B. Fowler, Phys. Rev. B **48**, 13238 (1993).
[15]D. C. Allan and M. P. Teter, J. Am. Ceram. Soc. **73**, 3247 (1990).
[16]R. H. Silsbee, J. Appl. Phys. **32**, 1456 (1961).
[17]J. K. Rudra, W. B. Fowler, and F. J. Feigl, Phys. Rev. Lett. **55**, 2614 (1985).
[18]T. Sander, C. T. Reindl, M. Giar, B. Eifert, M. Heinemann, C. Heiliger, and P. J. Klar, Phys. Rev. B **90**, 045203 (2014).
[19]A. F. Wright and J. S. Nelson, J. Appl. Phys. **92**, 5849 (2002).
[20]D. O. Scanlon, B. J. Morgan, G. W. Watson, and A. Walsh, Phys. Rev. Lett. **103**, 196405 (2009).
[21]L. Y. Isseroff and E. A. Carter, Chem. Mater. **25**, 253 (2013).
[22]E. P. Meagher and G. A. Lager, Can. Mineral. **17**, 77 (1979).
[23]S. V. Borisov, N. V. Pervukhina, and S. A. Magarill, J. Struc. Chem. **60**, 1946 (2019).
[24]L. K. Hudson, C. Misra, A. J. Perrotta, K. Wefers, and F. S. Williams, "Aluminum oxide," in *Ullmann's Encyclopedia of Industrial Chemistry* (Wiley - VCH, 2000).
[25]K. Kaneko, S. Fujita, T. Shinohe, and K. Tanaka, Jpn. J. Appl. Phys. **62**, SF0803 (2023).
[26]P. Hohn, S. Hoffman, J. Hunger, S. Leoni, F. Nitsche, W. Schnelle, and R. Kniep, Chem. Eur. J. **15**, 3419 (2009).
[27]A. Venzie, A. Portoff, M. Atavola, W. B. Fowler, J. Kim, D.-W. Jeon, J.-H. Park, and S. J. Pearton, Appl. Phys. Lett. **120**, 192101 (2022).
[28]Y. Lei and G. Wang, Scr. Mater. **101**, 20 (2015).
[29]S. Geller, J. Chem. Phys. **33**, 676 (1960).
[30]*Ultrawide Bandgap β-Ga_2O_3 Semiconductor: Theory and Applications*, edited by J. S. Speck and E. Farzana (AIP Publishing, Melville, NY, 2023).
[31]*Gallium Oxide: Materials Properties, Crystal Growth, and Devices*, edited by M. Higashiwaki and S. Fujita (Springer, Switzerland, 2020).
[32]M. Stavola, W. B. Fowler, A. Portoff, A. Venzie, E. R. Glaser, and S. J. Pearton, J. Appl. Phys. **135**, 101101 (2024).
[33]J. B. Varley, H. Peelaers, A. Janotti, and C. G. Van de Walle, J. Phys.: Condens. Matter **23**, 334212 (2011).
[34]A. Krytsos, M. Matsubara, and E. Bellotti, Phys. Rev. B **95**, 245202 (2017).
[35]P. Weiser, M. Stavola, W. B. Fowler, and Y. Qin, Appl. Phys. Lett. **112**, 232104 (2018).
[36]Y. Qin, M. Stavola, W. B. Fowler, P. Weiser, and S. J. Pearton, ECS J. Solid State Sci. Technol. **8**, Q3103 (2019).
[37]H. J. von Bardeleben, S. Zhou, U. Gerstmann, D. Skachkov, W. R. L. Lambrecht, Q. Ho, and P. Deák, APL Mater. **7**, 022521 (2019).
[38]D. Skachkov, W. R. L. Lambrecht, H. J. von Bardeleben, U. Gerstmann, Q. D. Ho, and P. Deák, J. Appl. Phys. **125**, 185701 (2019).
[39]J. M. Johnson, Z. Chen, J. B. Varley, C. M. Jackson, E. Farzana, Z. Zhang, A. R. Arehart, H.-L. Huang, A. Genc, S. A. Ringel, C. G. Van de Walle, D. A. Muller, and J. Hwang, Phys. Rev. X **9**, 041027 (2019).
[40]A. Karjalainen, V. Prozheeva, K. Simula, I. Makkonen, V. Callewaert, J. B. Varley, and F. Tuomisto, Phys. Rev. B **102**, 195207 (2020).
[41]W. B. Fowler, M. Stavola, Y. Qin, and P. Weiser, Appl. Phys. Lett. **117**, 142101 (2020).
[42]Y. K. Frodason, J. B. Varley, K. M. H. Johansen, L. Vines, and C. G. Van de Walle, Phys. Rev. B **107**, 024109 (2023).
[43]J. A. Kohn, G. Katz, and J. D. Broder, Am. Miner. **42**, 398 (1957).
[44]A. D. Becke, J. Chem. Phys. **98**, 5648 (1993).
[45]R. Krishnan, J. S. Binkley, R. Seeger, and J. A. Pople, J. Chem. Phys. **72**, 650 (1980).
[46]R. Dovesi, M. Causa', R. Orlando, and C. Roetti, J. Chem. Phys. **92**, 7402 (1990).
[47]J. E. Jaffe and A. C. Hess, Phys. Rev. B **48**, 7903 (1993).
[48]R. Nada, C. R. A. Catlow, C. Pisani, and R. Orlando, Model. Simul. Mater. Sci. Eng. **1**, 165 (1993).
[49]M. I. McCarthy and N. M. Harrison, Phys. Rev. B **49**, 8574 (1994).
[50]M. Catti, G. Valerio, R. Dovesi, and M. Causà, Phys. Rev. B **49**, 14179 (1994).
[51]R. Nada, C. R. A. Catlow, R. Dovesi, and C. Pisani, Phys. Chem. Miner. **17**, 353 (1990).
[52]M. Catti, R. Dovesi, A. Pavese, and V. R. Saunders, J. Phys.: Condens. Matter **3**, 4151 (1991).

[53]J. Muscat, Ph.D. Thesis (University of Manchester, 1999); J. Scaranto and S. Giorgianni, J. Mol. Struct. Theochem. **858**, 72 (2008). doi:10.1016/j.theochem.2008.02.027
[54]K. Doll and N. M. Harrison, Chem. Phys. Letters **317**, 282 (2000).
[55]R. Pandey, J. E. Jaffe, and N. M. Harrison, J. Phys. Chem. Solids **55**, 1357 (1994).
[56]G. Sophia, P. Baranek, C. Sarrazin, M. Rerat, and R. Dovesi, see from the CRYSTAL17 website:www.crystal.unito.it.